

UC Riverside

UC Riverside Previously Published Works

Title

Monomethylarsonous acid inhibited endogenous cholesterol biosynthesis in human skin fibroblasts

Permalink

<https://escholarship.org/uc/item/3s66t15m>

Journal

Toxicology and Applied Pharmacology, 277(1)

ISSN

0041-008X

Authors

Guo, Lei
Xiao, Yongsheng
Wang, Yinsheng

Publication Date

2014-05-01

DOI

10.1016/j.taap.2014.02.020

Peer reviewed

Published in final edited form as:

Toxicol Appl Pharmacol. 2014 May 15; 277(1): 21–29. doi:10.1016/j.taap.2014.02.020.

Monomethylarsonous Acid Inhibited Endogenous Cholesterol Biosynthesis in Human Skin Fibroblasts

Lei Guo¹, Yongsheng Xiao², and Yinsheng Wang^{2,*}

¹Environmental Toxicology Graduate Program, University of California, Riverside, CA 92521-0403

²Department of Chemistry, University of California, Riverside, CA 92521-0403

Abstract

Human exposure to arsenic in drinking water is a widespread public health concern, and such exposure is known to be associated with many human diseases. The detailed molecular mechanisms about how arsenic species contribute to the adverse human health effects, however, remain incompletely understood. Monomethylarsonous acid [MMA(III)] is a highly toxic and stable metabolite of inorganic arsenic. To exploit the mechanisms through which MMA(III) exerts its cytotoxic effect, we adopted a quantitative proteomic approach, by coupling stable isotope labeling by amino acids in cell culture (SILAC) with LC-MS/MS analysis, to examine the variation in the entire proteome of GM00637 human skin fibroblasts following acute MMA(III) exposure. Among the ~ 6500 unique proteins quantified, ~ 300 displayed significant changes in expression after exposure with 2 μ M MMA(III) for 24 h. Subsequent analysis revealed the perturbation of *de novo* cholesterol biosynthesis, selenoprotein synthesis and Nrf2 pathways evoked by MMA(III) exposure. Particularly, MMA(III) treatment resulted in considerable down-regulation of several enzymes involved in cholesterol biosynthesis. In addition, real-time PCR analysis showed reduced mRNA levels of select genes in this pathway. Furthermore, MMA(III) exposure contributed to a distinct decline in cellular cholesterol content and significant growth inhibition of multiple cell lines, both of which could be restored by supplementation of cholesterol to the culture media. Collectively, the present study demonstrated that the cytotoxicity of MMA(III) may arise, at least in part, from the down-regulation of cholesterol biosynthesis enzymes and the resultant decrease of cellular cholesterol content.

Keywords

Monomethylarsonous acid; quantitative proteomics; SILAC; FASP; *de novo* cholesterol biosynthesis

© 2014 Elsevier Inc. All rights reserved.

*To whom correspondence should be addressed: Department of Chemistry-027, University of California, Riverside, CA 92521-0403. Telephone: (951) 827-2700. Fax: (951) 827-4713. yinsheng.wang@ucr.edu.

Publisher's Disclaimer: This is a PDF file of an unedited manuscript that has been accepted for publication. As a service to our customers we are providing this early version of the manuscript. The manuscript will undergo copyediting, typesetting, and review of the resulting proof before it is published in its final citable form. Please note that during the production process errors may be discovered which could affect the content, and all legal disclaimers that apply to the journal pertain.

Introduction

Arsenic compounds are well-known environmental toxicants. As an abundant element in the earth crust, the presence of high levels of arsenic in naturally contaminated drinking water poses a widespread public health problem worldwide (Mandal and Suzuki, 2002). In addition, anthropogenic activities involving the use of arsenicals as pesticides, rodenticides, and fungicides further exacerbate the situation (Collotta *et al.*, 2013). Arsenic exposure was found to be associated with the development of respiratory irritations, dermal defects, neurological diseases, cardiovascular diseases and cancers (ATSDR, 2007). Many mechanisms have been proposed to account for the deleterious effects of arsenic species. In one mechanism, binding of As(III) with protein thiols is thought to disable critical proteins for regulating cell proliferation and metabolism (Kitchin and Wallace, 2008; Shen *et al.*, 2013). Additionally, arsenic was proposed to elicit its cytotoxic effects through the induction of oxidative stress (Kitchin, 2001; Flora, 2011).

Among the different arsenic species, monomethylarsonous acid [MMA(III)], a metabolite of inorganic arsenic, possesses the highest degree of toxicity. Biomethylation is the major mechanism for the metabolism of inorganic arsenic to produce MMA(III), though the role of this transformation in arsenic toxicity is under debate. Traditionally, methylation is viewed as the primary detoxification process since organic arsenic compounds can be detected in the urinary excretion (Marafante *et al.*, 1985). This, however, becomes questionable, as mounting evidence supports that organic arsenic compounds are more toxic than their inorganic counterparts both *in vitro* (Petrick *et al.*, 2000) and *in vivo* (Petrick *et al.*, 2001). Thus, a deep understanding of the modes of action for MMA(III) toxicity will help define the actual role of biomethylation in the toxification and detoxification of arsenic species.

Previous research about arsenic has focused on issues ranging from the detection and speciation of arsenic compounds to the interpretation of arsenic transport, metabolism, and toxicity (Mandal and Suzuki, 2002; Le *et al.*, 2004; Watanabe and Hirano, 2013). Genome-wide microarray analysis of human urothelial cells exposed with MMA(III) unveiled alterations of several biological processes and pathways including response to oxidative stress, enhanced cellular proliferation, anti-apoptosis, MAPK signaling, as well as inflammation (Medeiros *et al.*, 2012). Recent advances in mass spectrometry instrumentation and sample preparation methods provide the opportunity for conducting high-throughput and in-depth analysis of the alteration of the whole proteome (Aebersold and Mann, 2003). Therefore, we reason that assessing the changes in global protein expression upon MMA(III) exposure may offer a more complete picture about the mechanisms of its toxicity (Greenbaum *et al.*, 2003).

In this study, we employed liquid chromatography-tandem mass spectrometry (LC-MS/MS), together with stable isotope labeling by amino acids in cell culture (SILAC) (Ong *et al.*, 2002) and filter-aided sample preparation (FASP) (Wisniewski *et al.*, 2009), to examine the perturbation of cellular pathways induced by MMA(III) exposure. In total, we quantified approximately 6500 unique proteins, among which 198 and 105 were significantly increased and decreased, respectively, upon MMA(III) treatment. Notably, this study demonstrated, for the first time, that MMA(III) exposure resulted in down-regulation of multiple enzymes

engaged in *de novo* cholesterol biosynthesis. This finding, in combination with other experiments, supports that MMA(III) may exert its cytotoxic effect partly by inhibiting *de novo* cholesterol biosynthesis.

Methods

Cell Culture

All reagents unless otherwise stated were obtained from Sigma-Aldrich (St. Louis, MO), and all cell lines and cell culture reagents unless otherwise noted were from ATCC (Manassas, VA). MMA(III) and GM00637 cells were generously provided by Profs. X. Chris Le (University of Alberta) and Gerd P. Pfeifer (the City of Hope), respectively. GM00637 and HEK293T cells were cultured in Dulbecco's Modified Eagle's Medium (DMEM, ATCC) supplemented with 10% fetal bovine serum (FBS, Life Technologies, Grand Island, NY) and 100 IU/mL penicillin (ATCC). WM-266-4 cells were maintained under the above-mentioned conditions except that Eagle's Minimum Essential Medium (EMEM, ATCC) was used. Cells were cultured in a humidified atmosphere with 5% CO₂ at 37°C, with subculture at every 1–2 days.

MTT assay of dose-dependent cell viability was conducted using Cell Proliferation Kit 1 (Roche, Basel, Switzerland) and absorbance was recorded by Victor 2 plate reader (Perkin Elmer, Waltham, MA, Figure S1). Caspase 3 activity was examined by Western blot using caspase 3 antibody (Cell Signaling, Boston, MA) that detects the endogenous levels of full-length (35 kDa) and large fragments (17/19 kDa) of caspase-3 after cleavage at aspartic acid 175.

For SILAC labeling experiments, light lysine and arginine, or their stable isotope-labeled heavy counterparts ([¹³C₆,¹⁵N₂]-L-lysine and [¹³C₆]-L-arginine, Sigma), were added to the DMEM medium without L-lysine and L-arginine (Thermo Scientific, Rockford, IL) at concentrations following ATCC formulation to give the complete light and heavy DMEM media, respectively. GM00637 cells were maintained in the complete light or heavy DMEM medium with dialyzed FBS (Life Technologies, Grand Island, NY) for more than 10 days, corresponding to 5 cell doublings, to enable complete stable isotope incorporation into cells.

Monomethylarsonous Acid Treatment and Sample Preparation

GM00637 cells, at a density of ~5×10⁵ cells/mL in the light or, after complete heavy isotope incorporation, the heavy DMEM medium without dialyzed FBS, were exposed with 2 μM MMA(III) for 24 h. Cells were harvested by centrifugation at 300× *g* at 4°C for 5 min, washed with ice-cold phosphate-buffered saline (PBS) for three times, and lysed with 4% sodium dodecyl sulfate (SDS). Subsequently, the mixture was heated at 95°C for 5 min and centrifuged at 16,000× *g* at 4°C for 5 min with supernatant collected. The total protein concentration was measured by Bicinchoninic Acid Kit for Protein Determination (Sigma). For the forward SILAC experiment, the light labeled, MMA(III)-treated cell lysate was mixed at 1:1 ratio (w/w) with the heavy labeled, control cell lysate (Figure 1A), whereas the labeling and MMA(III) treatment were reversed in the reverse SILAC experiment.

Filter-aided Sample Preparation

The above equi-mass mixture of light and heavy lysates were reduced with dithiothreitol (DTT) and processed with the FASP procedure (Wisniewski *et al.*, 2009) for the removal of detergents (SDS) and tryptic digestion, where 30 kDa Microcon filtration devices were used (Millipore, Billerica, MA). Briefly, 400 µg lysate was loaded onto the filtration devices, washed with 8 M urea twice, and centrifuged at 14000× *g* for 15 min. After the centrifugation, the concentrates of proteins were alkylated with iodoacetamide (IAA), digested with trypsin (Promega, Madison, WI) at 37°C overnight, and the resulting peptides were collected by centrifugation of the filter units at 14000× *g* for 20 min.

Off-line Strong Cation Exchange (SCX) Fractionation and Desalting

The above protein digest was reconstituted in 0.1% formic acid (FA) and loaded onto a PolySulfoethyl A SCX column (9.4 × 200 mm, 5 µm, 200 Å, PolyLC, Columbia, MD). Peptides were eluted with a linear gradient of 0–500 mM ammonium acetate in 0.1% FA over 90 min, and collected every 4.5 min for a total of 20 fractions. Each fraction of the above protein digest was desalted and purified by the OMIX C₁₈ pipette tips (Agilent, Santa Clara, CA). Formic acid solution (0.1%) was added until the solution pH of the peptide sample reached ~ 4. Initially, the OMIX C₁₈ tips were hydrated with CH₃CN/H₂O (1:1, v/v), followed by equilibration with 0.1% formic acid. Subsequently, peptide samples were loaded onto the C₁₈ tip. After washing with 0.1% formic acid, bound peptides were eluted with CH₃CN/H₂O (1:1, v/v).

LC-MS and MS/MS

An LTQ-Orbitrap Velos mass spectrometer was utilized for the on-line LC-MS/MS analysis, which was equipped with a nanoelectrospray ionization source and coupled to an EASY n-LCII HPLC system (Thermo, San Jose, CA). The experimental conditions were the same as those described elsewhere (Guo *et al.*, 2013).

Database Search, Statistical Analysis and Pathway Analysis

Database search was conducted as previously published (Guo *et al.*, 2013). Briefly, the protein identification and quantification were performed using Maxquant (Cox and Mann, 2008), Version 1.2.2.5 based on the International Protein Index database, version 3.68. To obtain reliable results, the quantification of the protein expression ratio was based on three independent SILAC labeling experiments, which contained two forward and one reverse SILAC labelings. Statistical analysis for the protein expression ratios to define the significantly changed proteins was performed using Perseus 4.0 (Cox and Mann, 2008), where the “Significant A” value for each logarithmized ratio was calculated (Figure S2, Supporting Information). With a Benjamini-Hochberg threshold of 0.05, proteins with expression ratios [MMA(III)-treated/control] being greater than 1.30 or less than 0.70 fold were considered significantly altered. Follow-up pathway analysis of significantly changed proteins was carried out with the use of Gene Map Annotator and Pathway Profiler (GenMAPP-CS) (Salomonis *et al.*, 2007).

RNA Extraction and Quantitative Real-time PCR Analysis

Total RNA extraction of MMA(III)-treated and control GM00637 cells was performed using the Total RNA Kit 1 (VWR, Randor, PA), and reverse transcription using M-MLV reverse transcriptase (Promega, Madison, WI) and a poly(dT) primer. Subsequent qRT-PCR was conducted using iQ SYBR Green Supermix kit (Bio-Rad, Hercules, CA) and a Bio-Rad MyiQ thermal cycler. Gene-specific primers used for the analysis are listed in Table S1. Quantification of gene expression was performed with the comparative cycle threshold (*Ct*) method (Livak and Schmittgen, 2001), and the mRNA level of each gene was normalized to that of the *GAPDH* gene, which served as an internal control.

Exogenous Cholesterol Addition and Cell Proliferation Assay

The cholesterol-BSA complex was prepared for cholesterol incorporation into living cells as previously published (Martinez *et al.*, 1988). Briefly, 1% cholesterol in ethanol was mixed with water (1:1, v/v), which was then centrifuged at 2000× *g* for 10 min. Subsequently, the pellet was resuspended in an aqueous solution containing 0.25 M sucrose in 1 mM EDTA (pH 7.3), followed by a slow addition of 4 g bovine serum albumin (BSA, Sigma). The pH of the resultant solution was adjusted to 7.3 with Tris. After centrifugation at 12000× *g* for 10 min at 4°C, the supernatant was utilized for cholesterol rescue experiments.

GM00637, WM-266-4, and HEK293T cells were seeded in 24-well plates at a density of 1-1.5×10⁵ cells/mL. After a 12- or 24-h treatment with or without MMA(III) in the presence of 0, 30 or 60 mg/L cholesterol, or selected intermediates of cholesterol biosynthesis pathway, cells were stained with trypan blue and viable cells counted on a hemocytometer.

Extraction and Determination of the Cellular Cholesterol Level

Cells were lysed with CelLytic M buffer (Sigma), and total protein content was determined using Bradford Assay (Bio-Rad). Subsequently, cholesterol was extracted with chloroform:methanol:water (2:1.1:0.9, v/v/v) as previously published (Dong *et al.*, 2010). After centrifugation, the bottom chloroform layer was washed with a methanol-water mixture (5:4, v/v) for three times and collected. Total cholesterol level was determined by HPLC and normalized against the corresponding total protein content, as described previously (Guo *et al.*, 2013).

Results and Discussion

MMA(III) Treatment, Sample Preparation, Protein Identification, and Quantification

The toxic modes of action of arsenic, including MMA(III), have been extensively studied. Arsenic may exert its cytotoxic effect through binding with protein thiols to induce malfunction of critical proteins (Kitchin and Wallace, 2008; Shen *et al.*, 2013). In addition, exposure to MMA(III) may give rise to reactive oxygen species (ROS) in cells, which are capable of inducing DNA damage and triggering inflammatory response (Kitchin, 2001; Flora, 2011). However, MMA(III) may also act through other mechanisms. To investigate this, we utilized a quantitative proteomic technology to evaluate the MMA(III)-induced alteration of the global proteome in GM00637 human skin fibroblast cells. Initially, we determined the optimal dose of MMA(III) exposure by using a dose-dependent cell viability

assay. From MTT assay, a less than 9% cell death was observed for GM00637 cells following exposure to 2 μ M MMA(III) for 24 h. By contrast, a pronounced decline in cell survival (by ~30%) was induced by 8 μ M MMA(III) (Figure S1). This result is consistent with previous findings with other mammalian cells treated with MMA(III) (Petrick *et al.*, 2000; Charoensuk *et al.*, 2009; Shen *et al.*, 2009). In addition, treatment of 2 μ M MMA(III) did not induce apparent apoptosis, as revealed by lack of caspase 3 activation (See Western blot result in Figure S2). Therefore, we chose 2 μ M MMA(III) for the exposure experiment to minimize the apoptosis-induced perturbation of protein expression.

Upon complete SILAC labeling, GM00637 cells were treated with 2 μ M MMA(III) for 24 h and lysed with SDS. The light and heavy cell lysates were combined in equal mass, and subsequently purified and digested using the FASP protocol. After SCX fractionation, the resulting peptide mixtures were subjected to LC-MS/MS analysis.

Identification and quantification of the entire proteome were conducted using MaxQuant. Figure 2 shows the LC-MS/MS results of the peptide MLLNDFLNDQNR from 3-hydroxy-3-methylglutaryl-CoA synthase. The substantial decrease of this peptide in MMA(III)-exposed cells relative to control cells is evident from the MS results of samples obtained from both forward and reverse SILAC labeling experiments (Figure 2A and B), supporting the down-regulation of 3-hydroxy-3-methylglutaryl-CoA synthase. Additionally, the MS/MS results revealed the reliable identification of the corresponding light and heavy forms of the peptide (Figure 2C and D). In total, we were able to identify and quantify 7538 and 6543 proteins, respectively (Table S2). Among them, 4220, 1074, and 1249 could be quantified in all three, only two, and only one SILAC labeling experiment, respectively (Figure 1B).

Pathway Analysis for Significantly Altered Proteins upon MMA(III) Exposure

Figure 1C depicts the distribution of protein ratios representing alteration in protein expression triggered by MMA(III) exposure. The results showed that the expression of the majority of the quantified proteins (95.5%) was largely unchanged. To determine the threshold for screening significantly altered proteins, we utilized Perseus for the statistical analysis of the protein expression ratios (Cox and Mann, 2008). Significant A, as an outlier significance score, was calculated and plotted versus $\log_{10}(\text{Ratio})$ (Figure S3). Thus proteins with ratios 0.70- or 1.30-fold (Benjamini Hochberg FDR < 0.05) are categorized as significantly changed upon MMA(III) exposure; by using this criterion, we found that 105 and 198 proteins were significantly down- and up-regulated, respectively. All these proteins were analyzed in GenMAPP for pathway analysis, which revealed the down- and up-regulation of two and one pathways, respectively.

MMA(III)-inhibited *de novo* Cholesterol Biosynthesis

Pathway analysis revealed that cholesterol biosynthesis was significantly inhibited upon MMA(III) treatment (Figure 3). Particularly, we quantified 18 enzymes in this pathway, 8 of which were substantially (by 0.56–0.70 fold, Figure 3), and 6 modestly (by 0.71–0.83 fold), down-regulated. In addition, the expression of low-density lipoprotein receptor (LDL

receptor), a protein involved in the cellular uptake of LDL cholesterol (Defesche, 2004), was reduced by 0.66 fold.

To exploit if the diminished expression of the cholesterol biosynthesis enzymes arises from decreased mRNA expression of the corresponding genes, we performed real-time PCR analysis of five select genes (*HMGCS1*, *HMGCR*, *FDPS*, *FDFT1* and *DHCR7*) involved in this pathway. It turned out that the mRNA expression levels of all the measured genes were substantially decreased (by 0.61–0.79 fold, Figure 4), demonstrating that the reduced expression of these enzymes at the protein level stems primarily from transcriptional regulation.

Sterol regulatory element binding proteins (SREBPs) are the common transcription factors for the transcriptional activation of genes involved in cholesterol biosynthesis, including *HMGCS1* and *HMGCR* (Espenshade and Hughes, 2007). The abundance of SREBPs is regulated, in part, by the liver X receptor (LXR) and retinoid X receptor (RXR) heterodimers (Repa *et al.*, 2000). It was reported previously that arsenic trioxide can inhibit LXR/RXR via phosphorylation of RXR, thereby disrupting the nuclear receptor function of its binding partner (Mann *et al.*, 2005). Therefore, MMA(III) may deactivate the LXR/RXR heterodimer, thereby resulting in diminished SREBP synthesis, which subsequently gives rise to the down-regulation of genes involved in cholesterol biosynthesis.

MMA(III)-induced Reduction of Intracellular Cholesterol Level and Growth Inhibition could be Rescued by Exogenous Addition of Cholesterol

Given that several enzymes catalyzing cholesterol biosynthesis were down-regulated, we hypothesized that MMA(III) exposure may result in diminished production of cellular cholesterol. To explore this possibility, we measured the total cholesterol levels in GM00637 human skin fibroblast, WM-266-4 human melanoma, and HEK293T human embryonic kidney epithelial cells with or without MMA(III) exposure. Our results revealed significant declines of the cholesterol level (by 0.58–0.70 fold) in all the three cell lines following a 24-h exposure with 2 μ M MMA(III) (Figure 4B). This finding is in agreement with the MMA(III)-induced decreases, at both the mRNA and protein levels, of enzymes involved in the cholesterol biosynthesis. Thus, we conclude that MMA(III) inhibits *de novo* cholesterol biosynthesis. Along this line, it is worth noting that diminished cholesterol secretion from chest skin was found in individuals with arsenic skin lesions (Yousuf *et al.*, 2011).

On the basis of the above observations, we reasoned that the reduced endogenous cholesterol production may contribute to the cytotoxic effects of MMA(III). To test this, we assessed the MMA(III)-induced growth inhibition of cells and whether the inhibited cell proliferation could be abolished by the addition of exogenous cholesterol. Our results indeed showed that MMA(III) treatment caused significant inhibition of proliferation of GM00637, WM-266-4 and HEK293T cells and this inhibition could be restored by supplementation of cholesterol to the culture medium (Figure 5A–C). Consistently, the total cholesterol level returned to a comparable level as in control cells after a 24-h co-exposure with 2 μ M MMA(III) and 60 mg/L cholesterol (Figure 4B). Therefore, growth inhibition caused by

MMA(III) exposure of these cells may emanate primarily from the suppression of enzymes in cholesterol biosynthesis and the ensuing diminished *de novo* cholesterol production.

As a pivotal component of mammalian cell membrane, cholesterol plays a fundamental role in the maintenance of membrane permeability, fluidity, and membrane protein functions (Espenshade and Hughes, 2007). In addition, isoprenoid intermediates produced during cholesterol biosynthesis serve as lipid attachments for a variety of intracellular signaling molecules (Takemoto and Liao, 2001). Thus, maintaining homeostasis in cholesterol biosynthesis is of utmost importance in cell proliferation, differentiation and apoptosis. In this vein, aberrant cellular cholesterol level has been reported as the primary cause of cytotoxicity induced by Cr(VI) (Guo *et al.*, 2013) and some anti-cancer drugs (Dong *et al.*, 2011; Zhang *et al.*, 2012).

Aside from cholesterol, several important intermediates, including mevalonic acid (MVA), farnesyl pyrophosphate (FPP) and geranylgeranyl pyrophosphate (GGPP), are known to play pivotal roles in cell signaling and proliferation. Inhibition of such intermediates alone may induce cell death through pathways such as non-canonical activation of RhoA and Rac1 GTPases (Zhu *et al.*, 2013). Thus, there is some possibility that MMA(III), apart from perturbing intracellular cholesterol level, may also act through other pathways by inhibition of the aforementioned intermediates. However, supplementation with MVA, FPP or GGPP could not rescue the decreased cholesterol content or the growth inhibition arising from MMA(III) treatment (Figure 6). Therefore, we conclude that the MMA(III)-induced cytotoxicity emanates primarily from the depletion of cholesterol, the final product of the cholesterol biosynthesis pathway, rather than the reduced formation of intermediates produced in this pathway.

MMA(III)-induced Perturbation of Selenoprotein Synthesis

From the pathway analysis, we also observed the MMA(III)-induced perturbation of selenoproteins. In particular, MMA(III) treatment led to an increase of cytosolic thioredoxin reductase (TrxR1), but a decrease of selenoprotein M (Sel M). This finding is reminiscent of a previous study showing that exposure of human keratinocytes to MMA(III) could induce increase of TrxR1 and decrease of other small selenoproteins at both mRNA and protein levels (Ganyc *et al.*, 2007). Furthermore, several other studies have demonstrated the drop in activity of TrxR1 following MMA(III) exposure despite the overexpression of TrxR1, suggesting the strong inhibitory effect of MMA(III) on TrxR1 (Lin *et al.*, 1999; Meno *et al.*, 2009).

Selenoproteins possess critical functions in antioxidant defense (Davis *et al.*, 2012). For instance, it has been demonstrated that Sel M functions in reducing cellular ROS level and ROS-induced apoptotic cell death, as well as in maintaining cytosolic calcium level (Reeves *et al.*, 2010). Aberrant selenoprotein synthesis is known to be associated with damage of DNA, protein and lipids (Davis *et al.*, 2012). In this scenario, the decreased expression and/or activity of selenoprotein may result in a significant decline in the cells' ability to remove the ROS induced by MMA(III).

MMA(III)-induced Transcriptional Activation of Nrf2 Target Genes

In our quantitative proteomic experiment, we also found that the expression of multiple Nrf2 downstream genes was elevated following MMA(III) exposure. Nrf2 is a transcription factor known to mount a cellular response to defend cells against the deleterious effects of environmental toxicants (Kensler *et al.*, 2007). Natural Nrf2 activators, such as *tert*-butylhydroquinone and sulforaphane, act through the canonical Keap1-cysteine residue 151 (C151)-dependent mechanism (Lau *et al.*, 2013a), and these activators have been suggested for the therapeutic and dietary interventions against the adverse effects of arsenic (Wang *et al.*, 2007). Paradoxically, the activation of Nrf2 is also found to exert adverse effects. Along this line, distinct from the aforementioned natural Nrf2 activators, trivalent arsenic, including arsenite and MMA(III), may trigger Nrf2 activation through a distinct mechanism that is independent of C151 in Keap1 (Wang *et al.*, 2008). Particularly, arsenic-induced activation of Nrf2 antioxidant pathway was found to involve the accumulation of p62, which induces the dysregulation of autophagy and ultimately results in the sequestration of Keap1, thereby hindering the Keap1-Cullin 3 E3 ubiquitin ligase complex from functioning properly to ubiquitinate Nrf2 (Lau *et al.*, 2013b). This sustained activation has the potential to evoke arsenic toxicity instead of conferring protection.

We observed that several Nrf2 downstream targets, including glutamate-cysteine ligase and heme oxygenase-1, which are intracellular proteins involved in antioxidant defense, as well as NAD(P)H dehydrogenase [quinone] 1 (a.k.a. NAD(P)H:quinone oxidoreductase 1), which is a phase-II detoxifying enzyme, were up-regulated in human skin fibroblast cells upon MMA(III) treatment. This finding is in line with previous results showing that both inorganic As(III) and MMA(III) could trigger the Nrf2-dependent response in human bladder urothelial cells (Wang *et al.*, 2008). Thus, our results suggest that the previously reported As(III)-induced Nrf2 activation is not restricted to a particular cell type.

Conclusions

Human exposure to arsenic in drinking water is known to be correlated with the development of diverse human diseases (Smith *et al.*, 1992). MMA(III) is a toxic and stable arsenic metabolite, though the molecular mechanisms contributing to MMA(III) toxicity are not well understood. In the present study, we utilized an unbiased quantitative proteomic approach to evaluate the MMA(III)-induced perturbation of the entire proteome of GM00637 cells. Results from three independent sets of SILAC labeling experiments led to the quantification of 6543 unique proteins. Among them, 105 and 198 proteins were significantly down- and upregulated, respectively, following a 24-h exposure to 2 μ M MMA(III). Specifically, our study revealed that the cytotoxicity of MMA(III) may arise partly from the suppression of *de novo* cholesterol biosynthesis. In addition, the perturbation in selenoprotein synthesis and the activation of Nrf2 pathway may also lead to the adverse effect of MMA(III). Together, the results from the present study provide important new knowledge for the future clinical intervention towards MMA(III) exposure and, perhaps in general, arsenic exposure.

Supplementary Material

Refer to Web version on PubMed Central for supplementary material.

Acknowledgments

This work was supported by the National Institutes of Health (R01 ES019873).

Abbreviations

MMA(III)	monomethylarsonous acid
SILAC	stable isotope labeling by amino acids in cell culture
LC-MS/MS	liquid chromatography-tandem mass spectrometry
FASP	filter-aided sample preparation
DMEM	Dulbecco's Modified Eagle's Medium
EMEM	Eagle's Minimum Essential Medium
FBS	fetal bovine serum
PBS	phosphate-buffered saline
SDS	sodium dodecyl sulfate
DTT	dithiothreitol
IAA	iodoacetamide
FA	formic acid
GenMAPP	Gene Map Annotator and Pathway Profiler
LDL	low-density lipoprotein
SREBP	sterol regulatory element binding protein
LXR	liver X receptor
RXR	retinoid X receptor
TrxR1	thioredoxin reductase
Sel M	selenoprotein M
MVA	mevalonic acid
FPP	farnesyl pyrophosphate
GGPP	geranylgeranyl pyrophosphate

References

- Aebersold R, Mann M. Mass spectrometry-based proteomics. *Nature*. 2003; 422:198–207. [PubMed: 12634793]
- ATSDR. Toxicological Profile for Arsenic. Atlanta, GA: U.S. Department of Health and Human Services; 2007.

- Charoensuk V, Gati WP, Weinfeld M, Le XC. Differential cytotoxic effects of arsenic compounds in human acute promyelocytic leukemia cells. *Toxicol. Appl. Pharmacol.* 2009; 239:64–70. [PubMed: 19465042]
- Collotta M, Bertazzi PA, Bollati V. Epigenetics and pesticides. *Toxicol.* 2013; 307:35–41.
- Cox J, Mann M. MaxQuant enables high peptide identification rates, individualized p.p.b.-range mass accuracies and proteome-wide protein quantification. *Nat. Biotechnol.* 2008; 26:1367–1372. [PubMed: 19029910]
- Davis CD, Tsuji PA, Milner JA. Selenoproteins and cancer prevention. *Annu. Rev. Nutr.* 2012; 32:73–95. [PubMed: 22404120]
- Defesche JC. Low-density lipoprotein receptor--its structure, function, and mutations. *Semin. Vasc. Med.* 2004; 4:5–11. [PubMed: 15199428]
- Dong X, Xiao Y, Jiang X, Wang Y. Quantitative proteomic analysis revealed lovastatin-induced perturbation of cellular pathways in HL-60 cells. *J. Proteome Res.* 2011; 10:5463–5471. [PubMed: 21967149]
- Dong X, Xiong L, Jiang X, Wang Y. Quantitative proteomic analysis reveals the perturbation of multiple cellular pathways in Jurkat-T cells induced by doxorubicin. *J. Proteome Res.* 2010; 9:5943–5951. [PubMed: 20822187]
- Espenshade PJ, Hughes AL. Regulation of sterol synthesis in eukaryotes. *Annu. Rev. Genet.* 2007; 41:401–427. [PubMed: 17666007]
- Flora SJ. Arsenic-induced oxidative stress and its reversibility. *Free Radic. Biol. Med.* 2011; 51:257–281. [PubMed: 21554949]
- Ganyc D, Talbot S, Konate F, Jackson S, Schanen B, Cullen W, Self WT. Impact of trivalent arsenicals on selenoprotein synthesis. *Environ. Health Perspect.* 2007; 115:346–353. [PubMed: 17431482]
- Greenbaum D, Colangelo C, Williams K, Gerstein M. Comparing protein abundance and mRNA expression levels on a genomic scale. *Genome Biol.* 2003; 4:117. [PubMed: 12952525]
- Guo L, Xiao Y, Wang Y. Hexavalent chromium-induced alteration of proteomic landscape in human skin fibroblast cells. *J. Proteome Res.* 2013; 12:3511–3518. [PubMed: 23718831]
- Kensler TW, Wakabayashi N, Biswal S. Cell survival responses to environmental stresses via the Keap1-Nrf2-ARE pathway. *Annu. Rev. Pharmacol. Toxicol.* 2007; 47:89–116. [PubMed: 16968214]
- Kitchin KT. Recent advances in arsenic carcinogenesis: modes of action, animal model systems, and methylated arsenic metabolites. *Toxicol. Appl. Pharmacol.* 2001; 172:249–261. [PubMed: 11312654]
- Kitchin KT, Wallace K. The role of protein binding of trivalent arsenicals in arsenic carcinogenesis and toxicity. *J. Inorg. Biochem.* 2008; 102:532–539. [PubMed: 18164070]
- Lau A, Whitman SA, Jaramillo MC, Zhang DD. Arsenic-mediated activation of the Nrf2-Keap1 antioxidant pathway. *J. Biochem. Mol. Toxicol.* 2013a; 27:99–105. [PubMed: 23188707]
- Lau A, Zheng Y, Tao S, Wang H, Whitman SA, White E, Zhang DD. Arsenic inhibits autophagic flux, activating the Nrf2-Keap1 pathway in a p62-dependent manner. *Mol. Cell. Biol.* 2013b; 33:2436–2446. [PubMed: 23589329]
- Le XC, Lu X, Li X-F. Arsenic speciation. *Anal. Chem.* 2004; 76:26 A–33 A.
- Lin S, Cullen WR, Thomas DJ. Methylarsenicals and arsinothiols are potent inhibitors of mouse liver thioredoxin reductase. *Chem. Res. Toxicol.* 1999; 12:924–930. [PubMed: 10525267]
- Livak KJ, Schmittgen TD. Analysis of relative gene expression data using real-time quantitative PCR and the 2^{-C_t} Method. *Methods.* 2001; 25:402–408. [PubMed: 11846609]
- Mandal BK, Suzuki KT. Arsenic round the world: a review. *Talanta.* 2002; 58:201–235. [PubMed: 18968746]
- Mann KK, Padovani AMS, Guo Q, Colosimo AL, Lee H-Y, Kurie JM Jr, W HM. Arsenic trioxide inhibits nuclear receptor function via SEK1/JNK-mediated RXR α phosphorylation. *J. Clin. Invest.* 2005; 115:2924–2933. [PubMed: 16184197]
- Marafante E, Vahter M, Envall J. The role of the methylation in the detoxication of arsenate in the rabbit. *Chem. Biol. Interact.* 1985; 56:225–238. [PubMed: 4075449]

- Martinez F, Eschegoyen S, Briones R, Cuellar A. Cholesterol increase in mitochondria: a new method of cholesterol incorporation. *J. Lipid Res.* 1988; 29:1005–1011. [PubMed: 3183514]
- Medeiros M, Zheng X, Novak P, Wnek SM, Chyan V, Escudero-Lourdes C, Gandolfi AJ. Global gene expression changes in human urothelial cells exposed to low-level monomethylarsonous acid. *Toxicol.* 2012; 291:102–112.
- Meno SR, Nelson R, Hintze KJ, Self WT. Exposure to monomethylarsonous acid (MMA(III)) leads to altered selenoprotein synthesis in a primary human lung cell model. *Toxicol. Appl. Pharmacol.* 2009; 239:130–136. [PubMed: 19095002]
- Ong SE, Blagoev B, Kratchmarova I, Kristensen DB, Steen H, Pandey A, Mann M. Stable isotope labeling by amino acids in cell culture, SILAC, as a simple and accurate approach to expression proteomics. *Mol. Cell. Proteomics.* 2002; 1:376–386. [PubMed: 12118079]
- Petrick JS, Ayala-Fierro F, Cullen WR, Carter DE, Vasken Aposhian H. Monomethylarsonous acid (MMA(III)) is more toxic than arsenite in Chang human hepatocytes. *Toxicol. Appl. Pharmacol.* 2000; 163:203–207. [PubMed: 10698679]
- Petrick JS, Jagadish B, Mash EA, Aposhian HV. Monomethylarsonous acid (MMA(III)) and arsenite: LD(50) in hamsters and in vitro inhibition of pyruvate dehydrogenase. *Chem. Res. Toxicol.* 2001; 14:651–656. [PubMed: 11409934]
- Reeves MA, Bellinger FP, Berry MJ. The neuroprotective functions of selenoprotein M and its role in cytosolic calcium regulation. *Antioxid. Redox Signal.* 2010; 12:809–818. [PubMed: 19769485]
- Repa JJ, Liang G, Ou J, Bashmakov Y, Lobaccaro JM, Shimomura I, Shan B, Brown MS, Goldstein JL, Mangelsdorf DJ. Regulation of mouse sterol regulatory element-binding protein-1c gene (SREBP-1c) by oxysterol receptors, LXRalpha and LXRbeta. *Genes Dev.* 2000; 14:2819–2830. [PubMed: 11090130]
- Salomonis N, Hanspers K, Zambon A, Vranizan K, Lawlor S, Dahlquist K, Doniger S, Stuart J, Conklin B, Pico A. GenMAPP 2: new features and resources for pathway analysis. *BMC Bioinformatics.* 2007; 8:217. [PubMed: 17588266]
- Shen S, Lee J, Cullen WR, Le XC, Weinfeld M. Arsenite and its mono- and dimethylated trivalent metabolites enhance the formation of benzo[a]pyrene diol epoxide-DNA adducts in Xeroderma pigmentosum complementation group A cells. *Chem. Res. Toxicol.* 2009; 22:382–390. [PubMed: 19146383]
- Shen S, Li X-F, Cullen WR, Weinfeld M, Le XC. Arsenic binding to proteins. *Chem. Rev.* 2013; 113:7769–7792. [PubMed: 23808632]
- Smith AH, Hopenhayn-Rich C, Bates MN, Goeden HM, Hertz-Picciotto I, Duggan HM, Wood R, Kosnett MJ, Smith MT. Cancer risks from arsenic in drinking water. *Environ. Health Perspect.* 1992; 97:259–267. [PubMed: 1396465]
- Takemoto M, Liao JK. Pleiotropic effects of 3-hydroxy-3-methylglutaryl coenzyme A reductase inhibitors. *Arterioscler. Thromb. Vasc. Biol.* 2001; 21:1712–1719.
- Wang XJ, Sun Z, Chen W, Eblin KE, Gandolfi JA, Zhang DD. Nrf2 protects human bladder urothelial cells from arsenite and monomethylarsonous acid toxicity. *Toxicol. Appl. Pharmacol.* 2007; 225:206–213. [PubMed: 17765279]
- Wang XJ, Sun Z, Chen W, Li Y, Villeneuve NF, Zhang DD. Activation of Nrf2 by arsenite and monomethylarsonous acid is independent of Keap1-C151: enhanced Keap1-Cul3 interaction. *Toxicol. Appl. Pharmacol.* 2008; 230:383–389. [PubMed: 18417180]
- Watanabe T, Hirano S. Metabolism of arsenic and its toxicological relevance. *Arch. Toxicol.* 2013; 87:969–979. [PubMed: 22811022]
- Wisniewski JR, Zougman A, Nagaraj N, Mann M. Universal sample preparation method for proteome analysis. *Nat. Methods.* 2009; 6:359–362. [PubMed: 19377485]
- Yousuf AK, Misbahuddin M, Rahman MS. Secretion of arsenic, cholesterol, vitamin E, zinc from the site of arsenical melanosis and leucomelanosis in skin. *Clin. Toxicol.* 2011; 49:374–378.
- Zhang F, Dai X, Wang Y. 5-Aza-2'-deoxycytidine induced growth inhibition of leukemia cells through modulating endogenous cholesterol biosynthesis. *Mol. Cell. Proteomics.* 2012; 11:M111016915.
- Zhu Y, Casey PJ, Kumar AP, Pervaiz S. Deciphering the signaling networks underlying simvastatin-induced apoptosis in human cancer cells: evidence for non-canonical activation of RhoA and Rac1 GTPases. *Cell Death Dis.* 2013; 4:e568. [PubMed: 23559002]

Highlights

- MMA(III)-induced perturbation of the entire proteome of GM00637 cells is studied.
- Our quantitative proteomic approach revealed alterations of multiple cellular pathways.
- MMA(III) inhibits *de novo* cholesterol biosynthesis.
- MMA(III) perturbs Nrf2 pathway and selenoprotein synthesis.

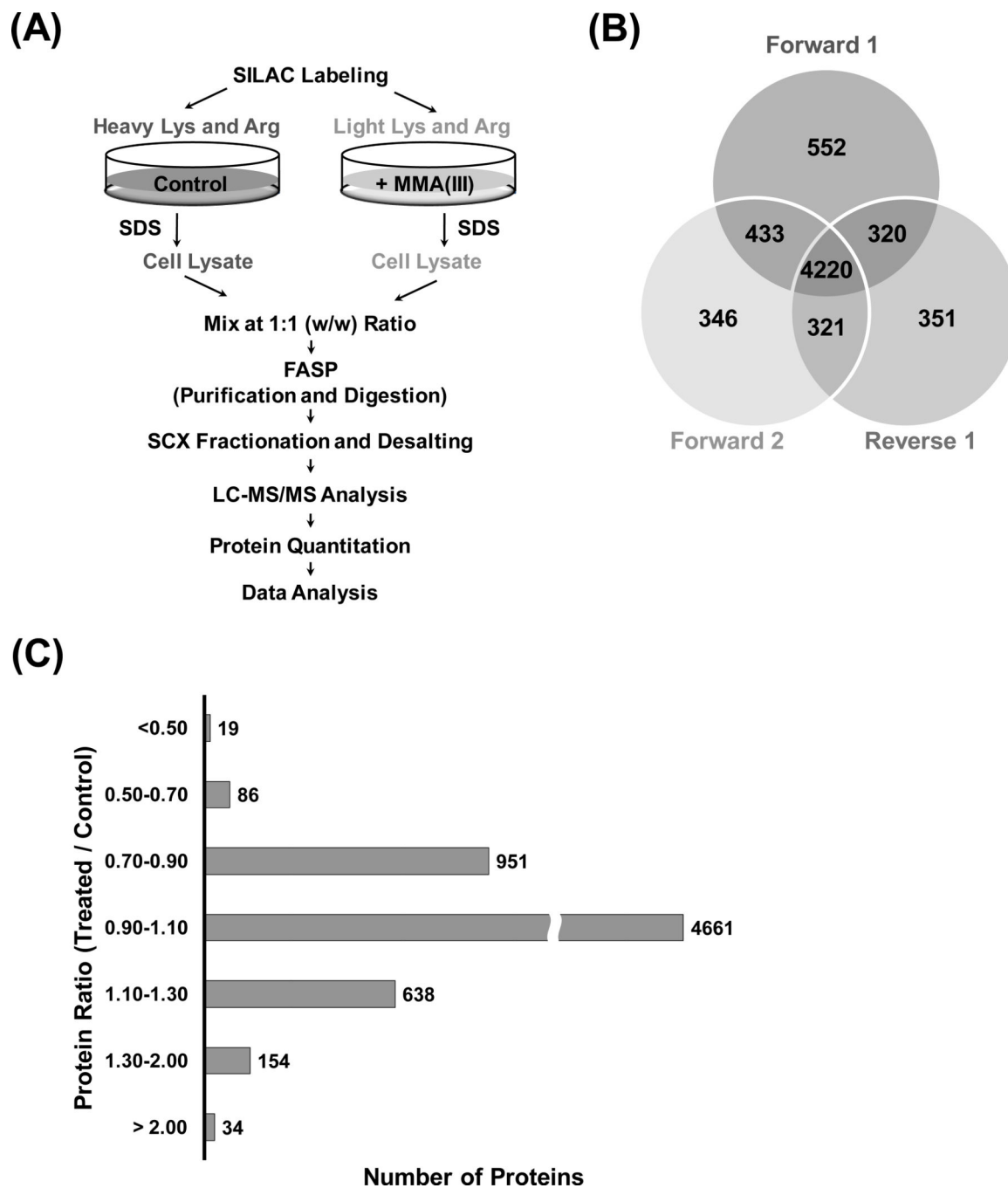


Figure 1. Quantitative analysis of global proteome perturbation induced by monomethylarsonous acid exposure

(A) Flowchart of forward SILAC coupled with LC-MS/MS analysis to reveal the alteration of protein expression in GM00637 cells following monomethylarsonous acid exposure. (B) Venn diagram depicting the number of proteins quantified in two forward and one reverse SILAC experiments. (C) The distribution of expression ratios for the quantified proteins.

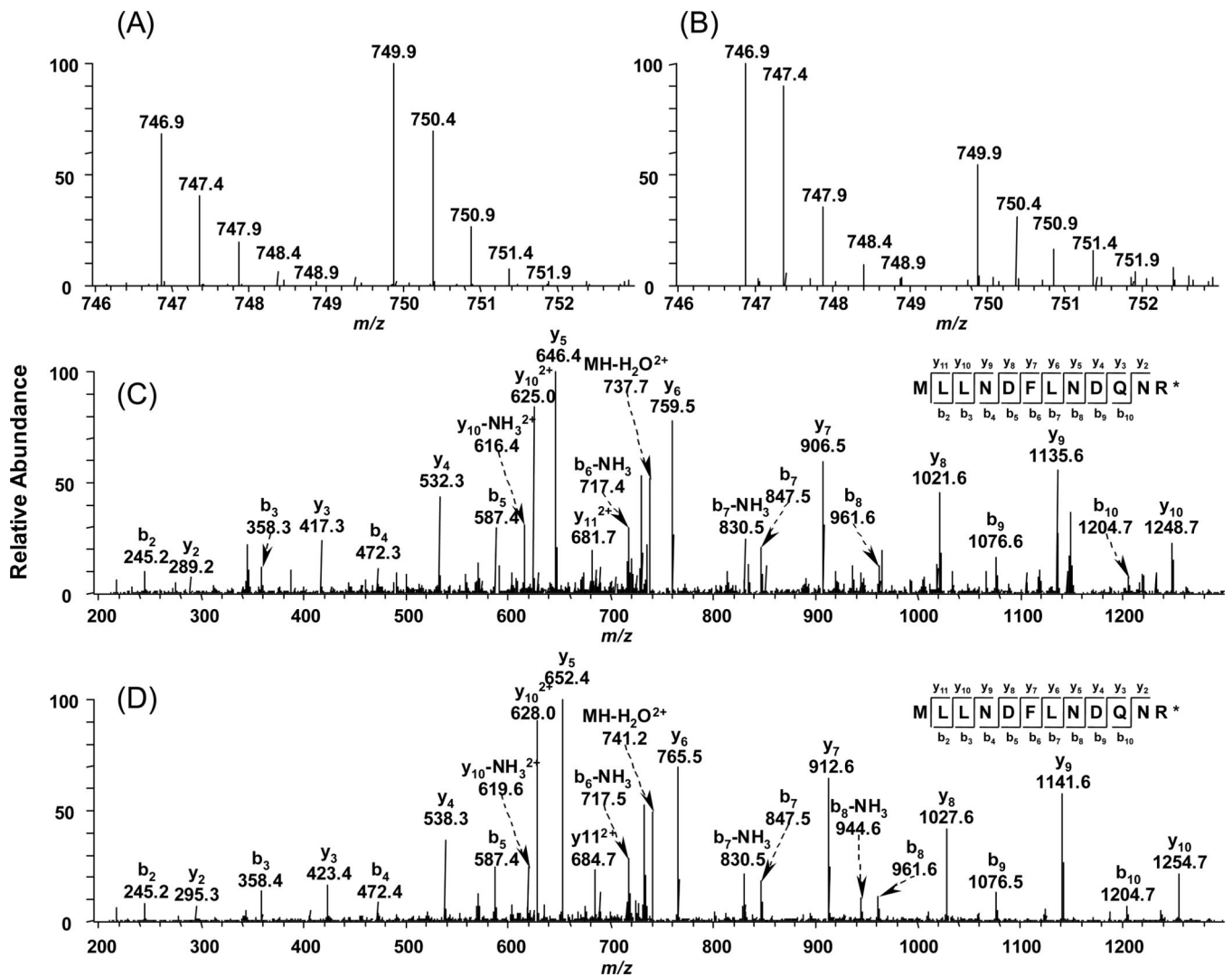


Figure 2. Representative ESI-MS and MS/MS demonstrating the MMA(III)-induced down-regulation of 3-hydroxy-3-methylglutaryl-CoA synthase
 Shown are the MS for the [M+2H]²⁺ ions of HMG-CoA synthase peptide MLLNDFLNDQNR and MLLNDFLNDQNR* (“R*” designates the heavy labeled arginine) from one forward (A) and one reverse (B) SILAC experiments. Shown in (C) and (D) are the MS/MS for the [M+2H]²⁺ ions of MLLNDFLNDQNR and MLLNDFLNDQNR*, respectively.

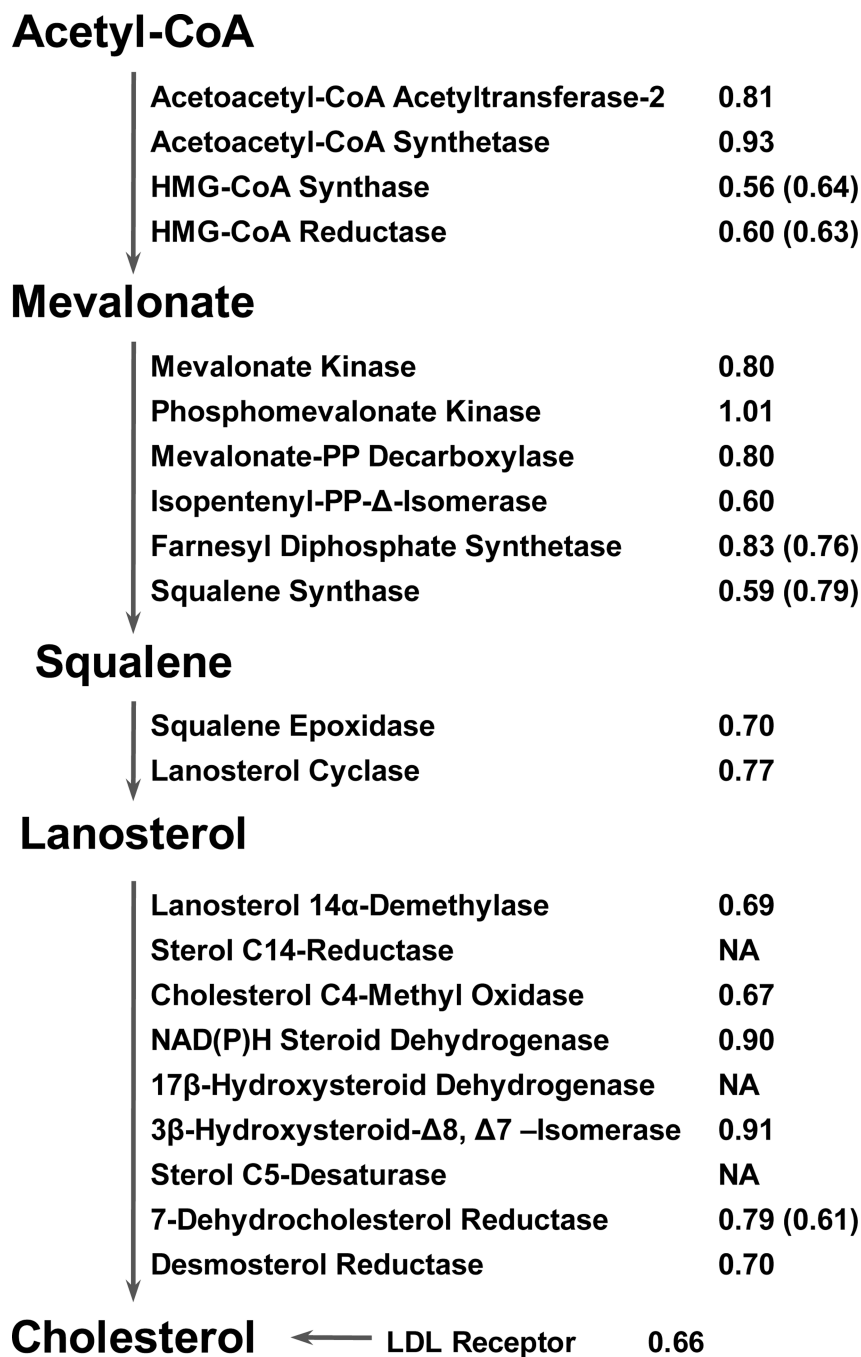


Figure 3. MMA(III) induced down-regulation of enzymes involved in key steps of *de novo* cholesterol biosynthesis

The expression ratios (MMA(III)-treated/control) of quantified enzymes are shown. 'NA', not available; these enzymes were not quantified in any set of the SILAC experiments. The relative mRNA expression levels assessed by real-time PCR are depicted in parenthesis. The values are the mean of results measured from three independent experiments.

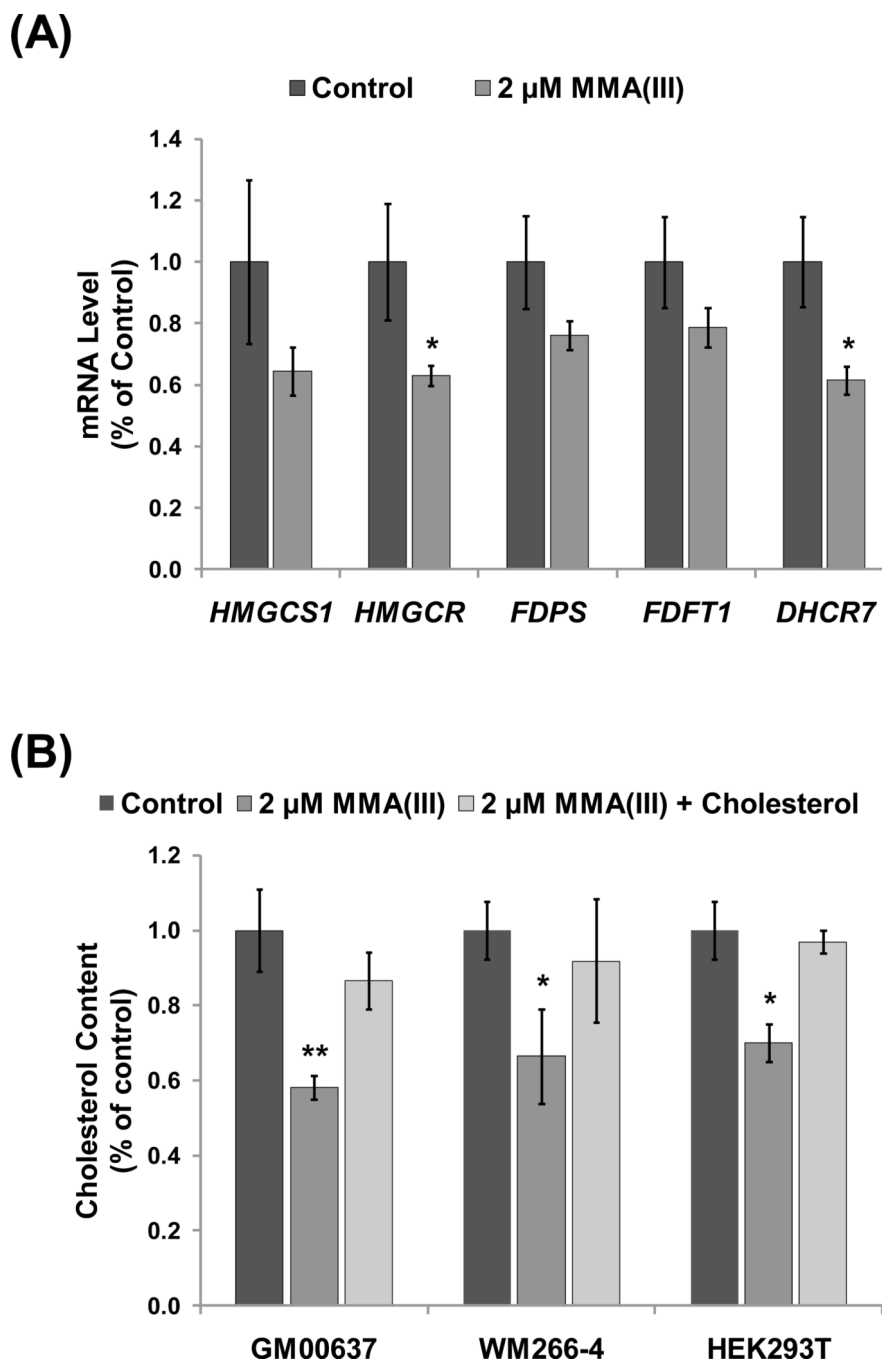


Figure 4. Monomethylarsonous acid perturbed the mRNA expression levels of genes involved *de novo* cholesterol biosynthesis (A) and suppressed cholesterol biosynthesis in cells (B)

Depicted in figure (A) are the histograms of relative mRNA expression levels of selected genes in the *de novo* cholesterol biosynthesis pathway in GM00637 cells with or without 2 μ M MMA(III) exposure for 24 h. (B) Cholesterol contents of GM00637, WM-266-4 and HEK293T cells that were untreated or treated for 24 h with 2 μ M MMA(III), alone or in combination with 60 mg/L cholesterol. Cellular cholesterol amount is normalized to that of the control. The values represent mean \pm S.D. of results obtained from three independent

experiments. ‘*’, $p < 0.05$; ‘**’, $p < 0.01$; ‘***’, $p < 0.001$. The p values were calculated by using unpaired two-tailed t -test.

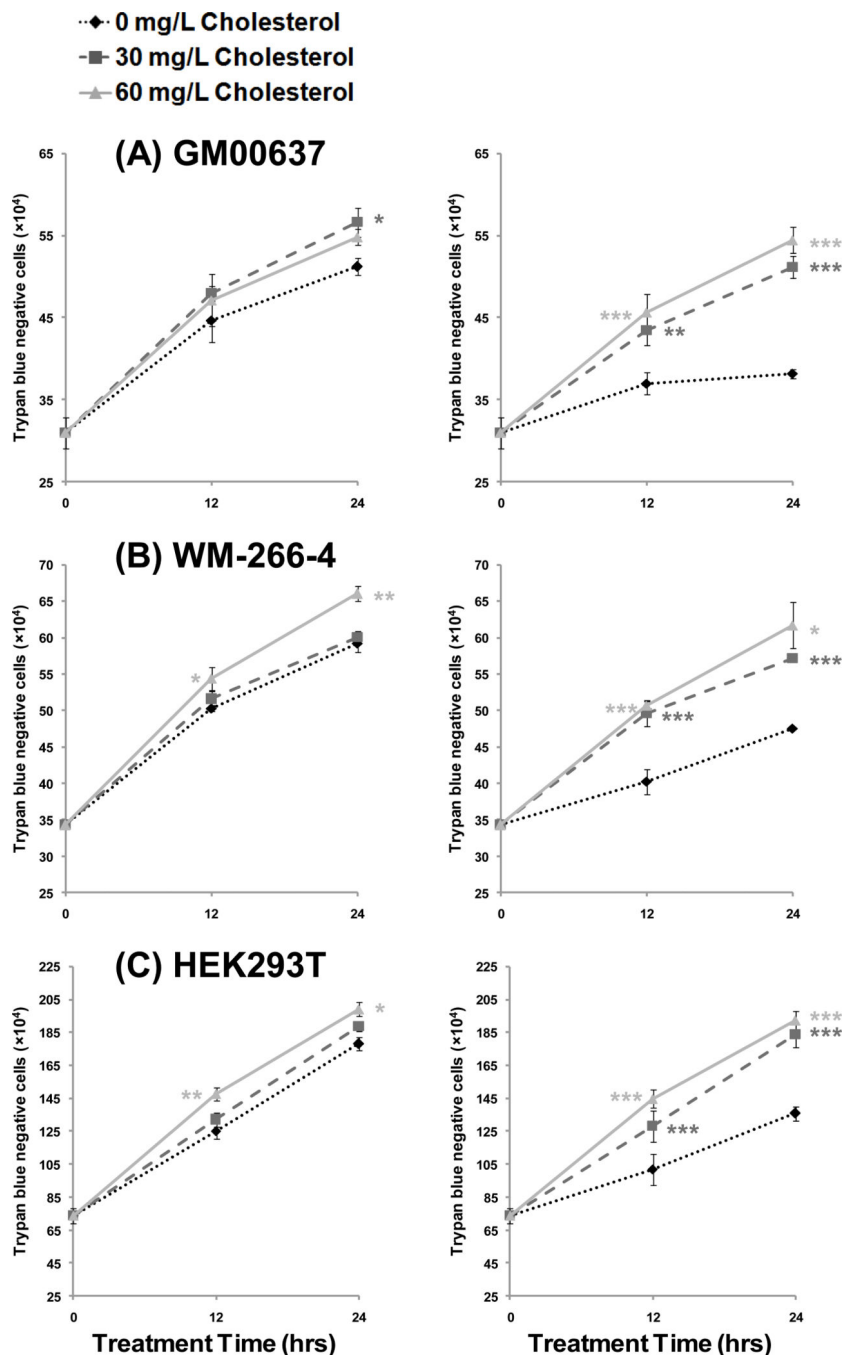
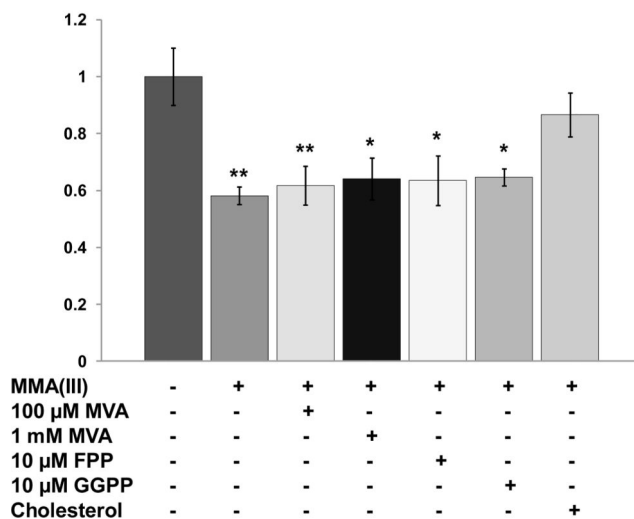


Figure 5. Monomethylarsonous acid-induced growth inhibition of cells could be abolished by addition of exogenous cholesterol

Number of trypan blue negative GM00637 (A), WM-266-4 (B) and HEK293T (C) cells measured by trypan blue exclusion assay after 12 or 24 h of treatment with 0 (black dotted line), 30 (dark grey dash line) or 60 mg/L (light grey solid line) cholesterol alone (left), or together with 2 μM MMA(III) (right). ‘*’, p < 0.05; ‘**’, p < 0.01; ‘***’, p < 0.001. The p values were calculated by using unpaired two-tailed *t*-test.

(A)



(B)

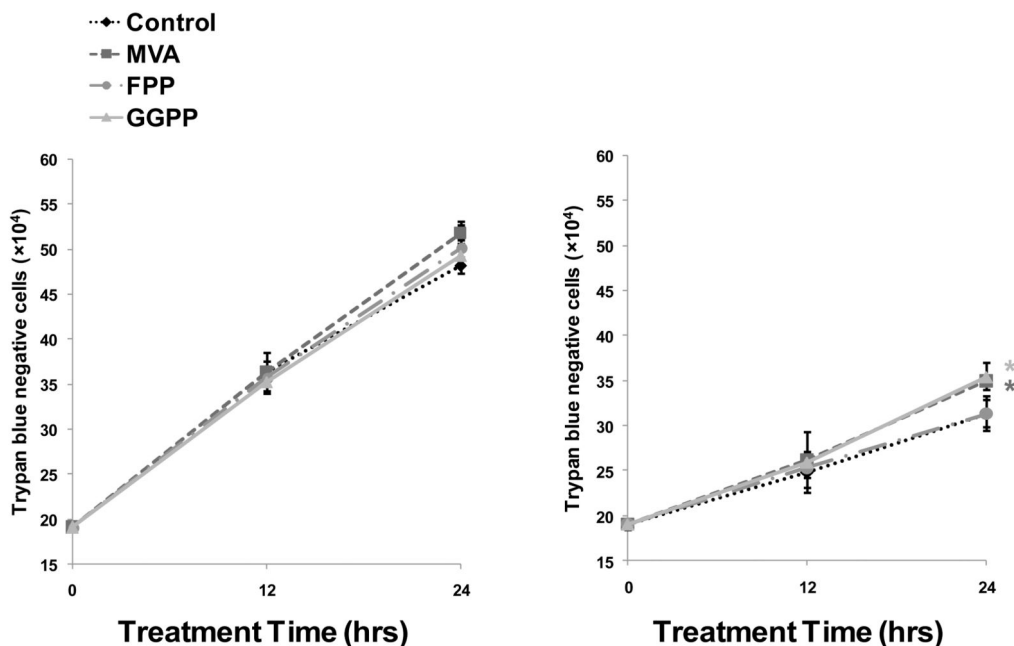


Figure 6. Monomethylarsonous acid-induced decline of cholesterol biosynthesis and growth inhibition of cells cannot be rescued by addition of intermediates of cholesterol biosynthesis pathway

(A) Cholesterol content of GM00637 cells that were untreated or treated for 24 h with 2 μM MMA(III), alone or in combination with intermediates of cholesterol biosynthesis pathway [mevalonic acid (MVA), farnesyl pyrophosphate (FPP) and geranylgeranyl pyrophosphate (GGPP)]. Cholesterol content is expressed as fold change of the value from control. (B) The amount of trypan blue negative GM00637 cells after 12 and 24 h of treatment with

intermediates alone (left), or together with 2 μ M MMA(III) (right). ‘*’, $p < 0.05$; ‘***’, $p < 0.01$. The p values were calculated by using unpaired two-tailed t -test.